RAPID COMMUNICATIONS

PHYSICAL REVIEW B VOLUME 43, NUMBER 7 1 MARCH 1991

Quantum diagrams and the prediction of new ternary quasicrystals

Karin M. Rabe
Department of Applied Physics, Yale University, New Haven, Connecticut 06520

A. R. Kortan and J. C. Phillips
AT&T Bell Laboratories, Murray Hill, New Jersey 07974

P. Villars
Villars Intermetallic Phases Databank, Postfach, Vitznau, CH-6354, Switzerland

(Received 18 October 1990)

We use the quantum-diagram technique to identify the chemical factors which favor quasicrystal formation. Expressed diagrammatically, these factors provide severe constraints on compositions at which quasicrystals or high-order rational approximants are likely to form. We outline several computerized search strategies which utilize the diagrammatic conditions to identify compositions for experimental investigation, and give examples of typical results.

So far, nine ternary stable and more than thirty metastable quasicrystalline phases have been discovered, but the total number of such phases is still unknown, as are the chemical factors which may cause these materials to have lower free energies (in some temperature ranges) than a phase-separated mixture of normal crystalline compounds. In this paper we discuss these questions theoretically. No theoretical method is known (and we suspect that probably no practical one exists) with the accuracy needed to resolve the free-energy differences between quasicrystals and related crystalline phases exactly. Instead, our analysis is designed to identify specific compositions where quasicrystalline structures are competitive in energy with conventional crystalline alternatives. Since the likelihood of quasicrystal formation is then significant, experimental investigation of such compositions should be rewarding.

Until now, most progress in understanding quasicrystalline materials has been made through investigation of related crystalline phases, which we will refer to as "corresponding compounds." Empirically, a corresponding compound has approximately the same composition as the quasicrystal and may occur as a second phase (with definite orientation relationships to the quasicrystal), as a transformation product of a metastable quasicrystal, or at the same composition but for different preparation procedures. For many corresponding compounds, with large unit cells and a high proportion of icosahedral local environments, there is clearly a strong structural relationship to quasicrystals. In fact, within a tiling description it is possible to view stable crystalline compounds such as α-$Si_2Mn_2Al_9$ and the *cI* 162 compound $LiCu_3Al_5$ as rational approximants to the metastable Al-Mn-Si and stable $LiCu_3Al_6$ quasicrystals, respectively.[1-4] For the $A_{15}Cu_{20}Al_{65}$ (A=Fe,Ru,Os) quasicrystals, however, there appear to be no stable corresponding compounds, and a metastable bcc phase $Fe_{15}Cu_{30}Al_{55}$ (a_0=2.93 Å) has only recently been identified.[5]

At finite temperature, the free-energy difference determines the relative stability of crystalline and quasicrystalline phases. Configurational entropy has been much discussed as a factor responsible for stabilizing quasicrystalline structures.[6] In fact, this contribution is very small and should only play an important role when other enthalpic factors are nearly equal.[7] Instead, the primary condition for quasicrystalline formation may be an energetic one which involves the same chemical factors that are responsible for crystalline stability. The complexity of the systems under consideration dictates the use of the quantum-diagram technique,[8-10] which provides a global organization of structure and stability data in the full intermetallic database of 25000 compounds. More specifically, in the construction of the three-dimensional quantum structural diagrams (QSD),[8,9] each compound is represented by a point whose coordinates are weighted averages of electronegativity ($\overline{\Delta X}$) and radius differences ($\overline{\Delta R}$) and valence-electron number ($\overline{N}_v$) of the constituent elements. In these diagrams, simply boundary surfaces can be drawn to separate compounds according to the local coordination environments present in the structure type, with an accuracy of 96% for a total of 5857 binary, ternary, and quaternary compounds. Different combinations of elemental parameters are used as coordinates in the construction of quantum formation diagrams (QFD),[10] which separate ternary-alloy systems that form ternary compounds from those that do not. For 7200 experimentally investigated systems, the accuracy of separation is 94%. Systems in or near the compound-nonforming region should contain conflicting contributions to total energies of crystalline compounds, generally resulting in the suppression or elimination of compound stability.

With the idea that local structure and stability are crucial issues in the formation of quasicrystals, we use QSD and QFD to look for regularities in the behavior of known quasicrystal-forming systems in the context of the full intermetallic database. As shown in Fig. 1 and Table I, the known stable quasicrystals $LiCu_3Al_6$,[11] $Ga_{20}Mg_{37}Zn_{43}$,[12] $Fe_{15}Cu_{20}Al_{65}$,[13] $Ru_{15}Cu_{20}Al_{65}$,[13] $Os_{15}Cu_{20}Al_{65}$,[13] $Cu_{15}Co_{20}Al_{65}$,[14] $Co_{15}Ni_{15}Al_{70}$,[14] and (Mn,Re)Pd_2Al_7 (Ref.

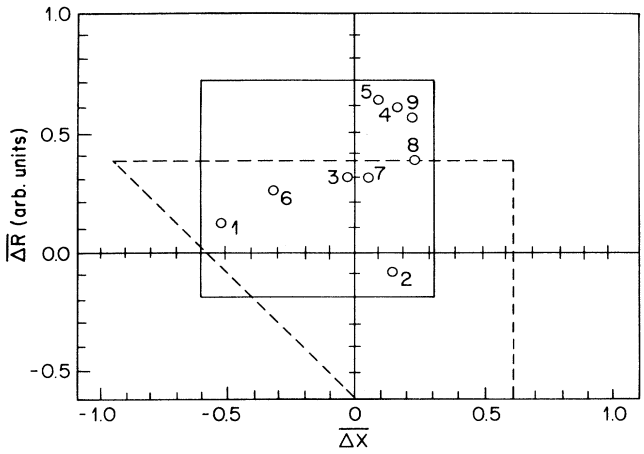

FIG. 1. The distribution of the nine stable quasicrystals on the QSD, projected along the $\overline{N}_v$ axis. Numbering of stable quasicrystals is as in Table I. The dashed line shows a portion of the boundary of the $\overline{\Delta X}$-$\overline{\Delta R}$ box defining the quasicrystal QSD condition of Ref. 18, based on *cI* 162 compounds and corresponding quasicrystals only. The solid line shows the box used in the present analysis. It is smaller and more accurate than the previous box because now nine stable quasicrystals are known rather than one.

14) are clustered on the QSD within the small box $-0.6 \leq \overline{\Delta X} \leq 0.03$, $-0.2 \leq \overline{\Delta R} \leq 0.7$. The compositions of most metastable quasicrystals also yield QSD coordinates in or nearly in this box. [These include $Al_{25}Mg_{36}Zn_{38}$, $Cu_9Mg_{36}Al_{55}$, $Ag_{15}Mg_{35}Al_{50}$, $Zn_{17}Li_{32}Al_{51}$, $AuLi_3Al_6$, $(Ag,Pd,Pt)_2Mg_{38}Al_{60}$, $(Au,Cu,Ni)_2Mg_{48}Al_{50}$, $Cr_{15}Cu_{20}Al_{65}$, $Mn_{15}Cu_{20}Al_{65}$, $Ni_{15}Cu_{20}Al_{65}$, $(Cr,Mn)_{20}Ge_{20}Al_{60}$, $Si_7Mn_{20}Al_{73}$, $Si_{20}Cr_{20}Al_{60}$, $Si_3Mn_{29}Ti_{68}$, and $V_{0.6}NiTi_{1.4}$; the only established exceptions are $U_{20}Si_{21}Pd_{59}$ and $SiNi_2Mn_3$.]

For information about the behavior of compounds in this region, we look at QSD structural separations of compounds which, like the established corresponding structure type *cI* 162, have four inequivalent local coordination environments. We studied 814 binary and ternary compounds in the four-environment structure types listed in Ref. 9. Of these 270, or 51%, of the 535 compounds with icosahedral environments fall in our small $\overline{\Delta X} - \overline{\Delta R}$ box, while only seven, or 2.5%, of the 279 nonicosahedral compounds have $\overline{\Delta X}$ and $\overline{\Delta R}$ values in this range, showing that this region (independent of $\overline{N}_v$) is primarily associated with the formation of icosahedral compounds. Most of the icosahedral compounds which lie outside our box have up to twice as large positive values of $\overline{\Delta R}$. It is evident that small values of $\overline{\Delta R}$ are even more important to quasicrystal formation than to icosahedral four-environment compound formation. On the other hand, in contrast to Hume-Rothery alloys,[15] $\overline{N}_v$ is of secondary importance to the phase stability of icosahedral structures, for our results show little correlation between $\overline{N}_v$ and icosahedral-compound formation and even less correlation of $\overline{N}_v$ with quasicrystal formation. The exception which proves the rule, (Fe,Ru,Os)-Cu-Al, may have a special structure, which we have discussed elsewhere[16] in connection with the anomalous transport properties of these quasicrystals.

The regularities on the QFD are also quite striking. As shown in Fig. 2, the nine stable quasicrystal alloy systems are clearly located either in or near the compound-nonforming region. All four systems falling well inside this region are notable in that they are among the few ($< 6\%$) known violators of QFD, with Fe-Cu-Al and Co-Cu-Al forming layered nonicosahedral compounds of (*tP* 40)-structure type, and Co-Ni-Al and Mn-Pd-Al forming compounds of (*cI* 112)- and (*cF* 16)-structure types, respectively.[17] Metastable quasicrystal alloy systems show a similar distribution on the QFD. This suggests that proximity to the compound-nonforming region is a suitable QFD condition for quasicrystal formation.

The organization of quasicrystals on the quantum diagrams in accordance with well-defined rules naturally lends itself to the development of severely selective computerized strategies for the prediction of new quasicrystals. One approach is to screen the inventory of ternary compounds in Ref. 16 requiring that their diagrammatic coordinates satisfy the QSD and QFD quasicrystal conditions. We have performed this search for the following sets of ternary compounds: (i) compounds in the (*cI* 162)-$Al_6Mn_{11}Zn_{11}$-structure type, which corresponds to the stable quasicrystals $LiCu_3Al_6$ and $Ga_{20}Mn_{37}Zn_{43}$; (ii) compounds in the (*cF* 116)-Th_6Mn_{23}-structure type, which has a large unit cell and a high degree of icosadedral coordination, but no established relationship to known quasicrystals; and (iii) compounds with more

TABLE I. The six diagrammatic coordinates used in the QSD and QFD analysis of the nine known stable quasicrystals. N_v' is a modified valence-electron number scale which includes the filled *d* electron shell in the near-noble metals Cu, Zn, Ag, Cd, Au, and Hg.

	$\overline{N}_v$	$\overline{\Delta R}$	$\overline{\Delta X}$	$\langle\lvert\Delta N_v'\rvert\rangle$	$\langle T_>/T_<\rangle$	$\langle\lvert\Delta R\rvert\rangle$
1. $Cu_{10}Li_{30}Al_{60}$	2.20	0.12	−0.52	6.67	2.15	0.29
2. $Ga_{20}Mg_{37}Zn_{43}$	2.20	−0.10	0.16	6.67	2.24	0.22
3. $Fe_{15}Cu_{20}Al_{65}$	3.35	0.30	−0.04	5.33	1.71	0.30
4. $Ru_{15}Cu_{20}Al_{65}$	3.35	0.59	0.15	5.33	2.29	0.62
5. $Os_{15}Cu_{20}Al_{65}$	3.35	0.62	0.07	5.33	2.81	0.65
6. $Cu_{15}Co_{20}Al_{65}$	3.90	0.25	−0.33	5.33	1.69	0.24
7. $Ni_{15}Co_{15}Al_{70}$	4.95	0.30	0.07	4.67	1.74	0.34
8. $MnPd_2Al_7$	4.80	0.37	0.25	4.67	1.74	0.52
9. $RePd_2Al_7$	4.80	0.56	0.26	4.67	2.66	0.67

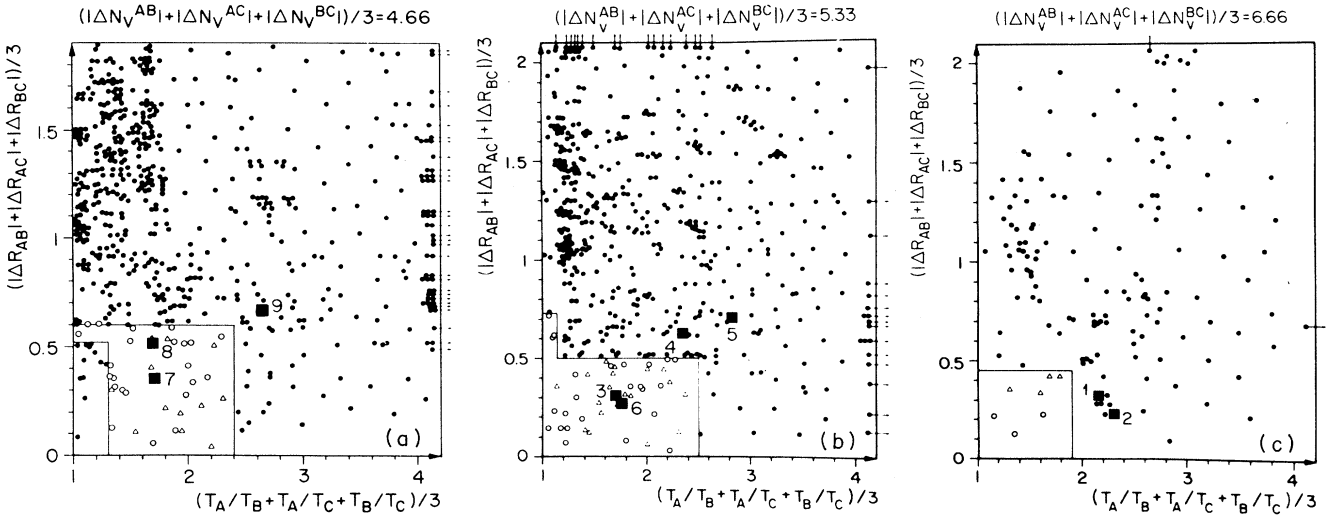

FIG. 2. (a) The $\langle|\Delta N_v|\rangle=4.67$ section of the ternary QFD (Ref. 10), showing the distribution of stable quasicrystals in relation to the boundary separating compound formation (solid circles) from compound nonformation (open circles and triangles). (b) Same as (a), with $\langle|\Delta N_v|\rangle=5.33$. (c) Same as (a), with $\langle|\Delta N_v|\rangle=6.67$.

than 75 atoms per unit cell which form in ternary-alloy systems in the compound-nonforming region of the QFD and have at least one binary compound-nonforming constituent pair. The results are given below.[18]

Considering how few large-unit-cell crystalline ternary phases have been studied, the use of known compounds as candidate corresponding compounds cannot form the basis of a comprehensive search strategy. Indeed, the most stable and well-ordered quasicrystals are expected to have only metastable corresponding compounds, and experimental investigation of that portion of the phase diagram would probably yield the quasicrystal more readily than the competing compound. Thus, it might at first seem that since a relatively small number of compositions can be experimentally examined, one would have to be remarkably fortunate to hit upon the correct ternary composition out of the enormous range of possibilities. In fact, with the use of quantum diagrams, a large number of element combinations (and stoichiometric ratios) can be quickly screened for those which satisfy the quasicrystal diagrammatic conditions. It was this approach which was used[19] to screen 2600 combinations of different groups of elements in the ratio 15:35:50, resulting in the correct prediction of the four metastable quasicrystals $Au_{15}Li_{35}Al_{50}$, $Zn_{15}Li_{35}Al_{50}$, $Ag_{15}Mg_{35}Al_{50}$, and $Ga_{15}Mg_{35}Zn_{50}$.[20] Refinement of the latter composition yields the second stable quasicrystal $Ga_{20}Mg_{37}Zn_{43}$.[12] We carried out a similar procedure based on the ratio 15:20:65 (transition metal–near-noble metal–p element) with the condition that the QSD coordinates lie within ranges centered on the prototype quasicrystals $Fe_{15}Cu_{20}Al_{65}$, $Os_{15}Cu_{20}Al_{65}$, and $Ru_{15}Cu_{20}Al_{65}$. This screening reduces 3780 possible combinations to a short list of fewer than thirty.[21] For most of these compositions, there are no previously known nearby compounds and even information about the ternary-phase diagrams is very limited,[17] giving the diagrammatic analysis a crucial role in their selection for examination. Further investigations in progress include a similar search based on the addition of a third element to the prototype crystals[15,17] $PdAl_4$ and Sr_9Mg_{38}.

In summary, quasicrystals show strong regularities with respect to the full database of known intermetallic compounds. The diagrammatic conditions for quasicrystal formation have a simple physical interpretation in terms of local coordination environment and tendency to compound formation. It is expected that severely selective diagram-based searches will play an increasingly important role in the expansion of the quasicrystal database, which in turn is crucial in improving the understanding of the physics of quasicrystallinity in real materials.

[1]V. Elser and C. L. Henley, Phys. Rev. Lett. **55**, 2883 (1985); C. L. Henley and V. Elser, Philos. Mag. B **53**, L59 (1986).

[2]P. Guyot and M. Audier, Philos. Mag. B **52**, L15 (1985); M. Audier and P. Guyot, *ibid.* **53**, L43 (1986).

[3]V. Kumar, D. Sahoo, and G. Athithan, Phys. Rev. B **34**, 6924 (1986).

[4]M. Audier, P. Sainfort, and B. Dubost, Philos. Mag. B **54**, L105 (1986).

[5]S. Ebalard and F. Spaepen, J. Mater. Res. **5**, 62 (1990).

[6]Katherine J. Strandburg, Phys. Rev. B **40**, 6071 (1989), and references therein.

[7]Katherine J. Strandburg, Lei-Han Tang, and Marko V. Jaric, Phys. Rev. Lett. **63**, 314 (1989); M. Widom, D. P. Deng, and C. L. Henley, *ibid.* **63**, 310 (1989).

[8]P. Villars and F. Hulliger, J. Less-Common Met. **132**, 289 (1987).

[9]P. Villars, K. Mathis, and F. Hulliger, in *Structures of Binary Compounds,* edited by F. de Boer and D. Pettifor (North-

Holland, Amsterdam, 1989), Vol. 2, p. 1.

[10]P. Villars, J. Less-Common Met. **119**, 175 (1986).

[11]P. Sainfort and B. Dubost, J. Phys. (Paris) Colloq. **47**, C3-321 (1986); W. A. Cassada, G. J. Shiflet, and S. J. Poon, Phys. Rev. Lett. **56**, 2276 (1986).

[12]W. Ohashi and F. Spaepen, Nature (London) **230**, 555 (1987).

[13]A. P. Tsai, A. Inoue, and T. Masumoto, Jpn. J. Appl. Phys. Pt. 2 **26**, L1505 (1987); K. Hiraga, B. P. Zhang, M. Hirabayashi, A. Inoue, and T. Masumoto, *ibid.* **27**, L951 (1988); A. P. Tsai, A. Inoue, and T. Masumoto, *ibid.* **27**, L1587 (1988).

[14]A. P. Tsai, A. Inoue, and T. Masumoto, Mater. Trans., JIM **30**, 463 (1989); A. P. Tsai, A. Inoue, and Y. Yokoyama, and T. Masumoto, *ibid.* **31**, 98 (1990).

[15]J. Friedel, Helv. Phys. Acta A **61**, 538 (1988).

[16]J. C. Phillips and K. M. Rabe (unpublished).

[17]P. Villars and L. D. Calvert, *Pearson's Handbook of Crystallographic Data for Intermetallic Phases* (American Society of Metals, Metals Park, OH, 1985).

[18]In this reference, quasicrystal predictions are listed in roman typeface for experimentally confirmed quasicrystals, and in italics for outstanding predictions: (i) $Cu_8Mg_{40}Al_{52}$, $Al_{21}Mg_{39}Zn_{40}$, $Zn_{17}Li_{32}Al_{51}$, $Ga_{16}Li_{32}Zn_{52}$, $Cu_{11}Li_{32}Al_{57}$, $Ga_{16}Mg_{32}Zn_{52}$; (ii) $Hf_6Si_7Co_{16}$, $Zr_6Si_7Co_{16}$, $Mg_6Si_6Cu_{16}$, $Mg_6Ge_7Ni_{16}$, $Mn_6Ni_{16}Ge_7$, $Mn_6P_7Ni_{16}$, $Mn_6Si_7Ni_{16}$, $V_6Si_7Ni_{16}$; (iii) o^*380 $Mn_3Cu_5Al_{11}$, oF 224 $PbGa_2Se_4$, cF 184 $Al_{20}Cr_2$(*Dy, Er, Ho, La, Y, Nd*), cF 184 $Al_{20}V_2$(*Dy, Gd, Nd*), cI 162 $Al_6Mg_{11}Zn_{11}$, oP 160 $Sb_4Pb_5S_{11}$, oC 152 $Zn_2Mn_3Al_{11}$, oC 152 $Cu_2Mn_{32}Al_{20}$, cF 112 $La_2Si_3Fe_{23}$, mC 104 $Pb_3Sb_8S_{15}$, cF 96 $Zn_{11}Pb_{17}Cd_{22}$, mP 90 $As_6Pb_{14}S_{23}$, cF 84 $Cr_4Si_4Al_{13}$, oP 76 $Mo_3Si_8Mn_8$.

[19]P. Villars, J. C. Phillips, and H. S. Chen, Phys. Rev. Lett. **57**, 3085 (1986).

[20]H. S. Chen, J. C. Phillips, P. Villars, A. R. Kortan, and A. Inoue, Phys. Rev. B **35**, 9326 (1987).

[21]Quasicrystal predictions $A_{15}B_{20}C_{65}$ are listed for brevity as *A-B-C* with their prototype stable quasicrystal and the $(\overline{\Delta X},\overline{\Delta R})$ range into which they fall. Conventions are as in Ref. 17. $Fe_{15}Cu_{20}Al_{65}$ $(-0.1,0.0)\times(0.25,0.35)$: Co-Ag-Al, Co-Au-Al, Cr-Au-Pb, Fe-Ag-Al, Fe-Cd-Al, Mn-Ni-Sb, Rh-Ag-Pb, Rh-Au-Pb, Ru-Cu-Pb, Ti-Cd-Pb, V-Ag-Bi, W-Ag-Tl, W-Cu-Tl. (Os or Ru)$_{15}Cu_{20}Al_{65}$ $(0.0,0.2)\times(0.55,0.65)$: Cr-Au-Al, Ir-Ag-Al, Ir-Cu-Al, Ir-Ni-Al, Ir-Pd-Al, Ir-Zn-Al, Mo-Zn-Al, Os-Ni-Al, Re-Cu-Al, Rh-Ag-Al, Rh-Au-Al, Rh-Cd-Al, Ru-Ag-Al, Ru-Cd-Al, Ru-Zn-Al, Ti-Cd-Al.